Signal-to-noise ratio analysis and optimization on digital readout integrated circuit for microbolometric focal plane array

XIQU CHEN*, MENGYUN WANG, CHAO FANG
School of Electrical & Electronic Engineering, Wuhan Polytechnic University, Wuhan, China

The signal-to-noise ratio of readout integrated circuit is a vital parameter for microbolometric focal plane array to decide its noise equivalent temperature difference, which often restricts the temperature resolution of infrared image system. The noise and responsivity of microbolometric focal plane array with digital readout integrated circuit are theoretically analyzed, based on which the theoretical signal-to-noise ratio expression is achieved. According to the theoretical expression, a new kind of optimized digital readout integrated circuit for microbolometric focal plane array is proposed in this paper. The optimized digital readout integrated circuit is utilized to digitalize the infrared response signal with pulse frequency modulation not conventional pulse width modulation. Theoretical discussion and experimental verification make it known that the optimized digital readout integrated circuit has excellent performance characteristics such as low noise and high responsivity.

1. Introduction

For its more powerful anti-interference capacity than that of classical analog readout integrated circuit for focal plane array, the digital readout integrated circuit on-chip is needed for modern focal plane array [1,2]. At the same time, because of the fabricating process of microbolometer array is completely compatible with the manufacturing process of current CMOS (Complementary Metal Oxide Semiconductor) integrated circuit, the microbolometric focal plane array integrated with sensor array and on-chip digital signal readout circuit dominates in uncooled infrared image detectors [3-7]. The operating principle of current microbolometric focal plane array can be explained as follows. When the microbolometer array is irradiated by infrared radiation, the resistance variations of all the microbolometers in the array due to the microbolometer temperature increases are often transformed into corresponding photo-generated currents, and these photo-generated currents can be separately accumulated onto a list of integration capacitors to form analog infrared pixel response voltages [8,9]. These analog response voltages are normally digitalized through some on-chip ADCs (Analog-to-Digital Converters) to be output as infrared digital pixel response signals [10,11].

The output signal-to-noise ratio of the microbolometric focal plane array is critically important because it represents the quality of the infrared image signals from the microbolometric focal plane array [12-14], which is basically determined by the thermal characteristics of microbolometer array and the electronic features of the readout integrated circuit.

Since the microbolometer thermal sensitivity and structure are relatively stable, the development of CMOS readout integrated circuit can effectively improve the performance properties of microbolometric focal plane array such as signal-to-noise ratio. There are several kinds of stochastic noises in the microbolometric focal plane array with analog readout integrated circuit mainly including thermal and excess noises of microbolometer and excess noise of the CMOS readout integrated circuit [15]. All these kinds of noises are dependent on the bandwidth of the readout integrated circuit, which indicates that the CMOS readout integrated circuit should be designed with low-noise scheme.

The theoretical expressions of vital stochastic noises associated with the bandwidths of CMOS readout integrated circuit are introduced in some paper [15,16], and the infrared responsivity of microbolometric focal plane array is theoretically discussed in our previous papers [17,18]. However, these theoretical expressions of noises and responsivity are given out for microbolometric focal plane array with conventional analog readout integrated circuit and are not practical for modern microbolometric focal plane array with digital readout integrated circuit. In this paper, the theoretical signal-to-noise ratio based on the mathematical expressions of noises and responsivity is provided for modern microbolometric focal plane array, according to which a new optimization method for digital CMOS readout integrated circuit is proposed for next-generation high-performance microbolometric focal plane array.

2. Signal-to-noise ratio analysis

The block diagram of pixel signal channel for single microbolometer in current microbolometric focal plane array is shown in Fig. 1, which consists of two key parts: the microbolometer and the digital readout integrated circuit including the photo-generated current integration circuit and the ADC. There are two kinds of predominant noises from the microbolometer, one is Johnson noise and the other is 1/f noise. The total excess noise of the digital readout integrated circuit is entirely contributed from the photo-generated current integration and ADC circuits because of their CMOS insulator materials. In consideration that the electronic noise of readout integrated circuit should be significantly less the noise of the microbolometer, the excess noise of the digital readout integrated circuit can be ignored by using some electronic engineering technologies such as low-noise integration preamplifier or noise correlated double sampling circuit [19]. Nevertheless, the quantization noise caused by the ADC is not correlated with Johnson noise and 1/f noise from the microbolometer and the total excess noise of the digital readout integrated circuit, and cannot be ignored for its magnitude. Thus, these three kinds of major stochastic noises: Johnson noise, 1/f noise and quantization noise will be introduced and discussed as follows.
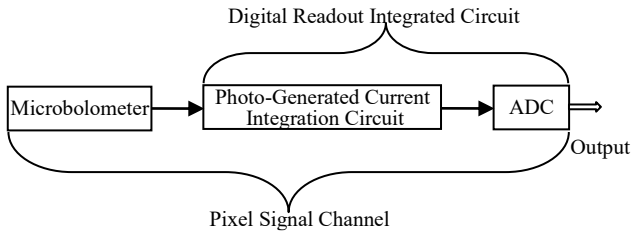

Fig. 1. Signal channel for single microbolometer

2.1. Noise analysis

The typical simple digital readout integrated circuit for a microbolometer is shown in Fig. 2, in which all the integrated circuit except for the microbolometer is shared by all the microbolometers in one column in a pratical microbolometric focal plane array. When the row selecting switch S_1 is turned on after the integration capacitor C is discharged by the reset switch S_0, the photo-generated current I_P is integrated onto the integration capacitor to form an infrared response voltage after a certain integration time t_{int} through the amplifier A. The infrared response voltage is converted into digital output D_{out} by the ADC.
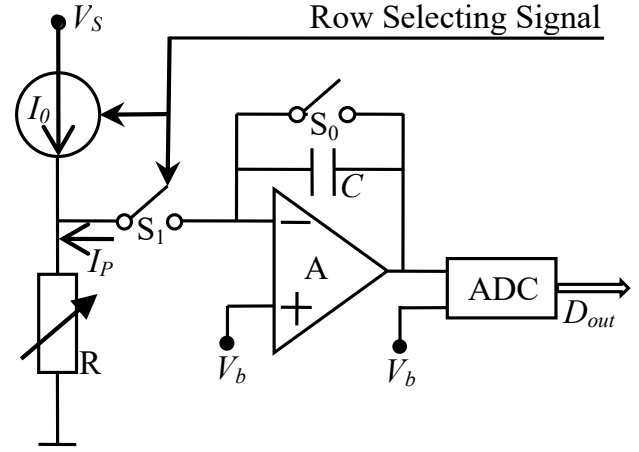

Fig. 2. Simple digital readout integrated circuit

The Johnson noise is resulted from the thermal agitation of charge carriers in the microbolometer, and its mean-square current in a 1 Hz bandwidth within the noise bandwidth Δf can be represented as

$$I_J^2 = \frac{4KT}{R},\qquad(1)$$

where K is the Boltzmann constant, and T and R are the microbolometer temperature and resistance value respectively. The 1/f noise is uncorrelation with the Johnson noise, and its mean-square current in a 1 Hz bandwidth within the noise bandwidth is

$$I_{1/f}^2 = \frac{V_v^2 k}{R^2 f},\qquad(2)$$

where V_v is the volume of the microbolometer, k is the 1/f noise parameter, and f is the noise frequency between the lower cut-off frequency f_1 and the noise upper frequency f_2. It is worth noting that Δf is equal to $f_2 - f_1$.

If the maximum integration voltage on the integration capacitor C is V_{max} and the ADC is b bits, the relationship between digital output and analog input of the ADC is illustrated in Fig. 3, from which it can be derived that the digital output corresponding to m bits is

$$D_{out} = \frac{V_{max}}{2^b} \times 2^m = 2^{m-b} V_{max},\qquad(3)$$

and the quantization range of analog input voltage is

$$[(2^{m-b} - 2^{-b-1})V_{max}, (2^{m-b} + 2^{-b-1})V_{max}].\qquad(4)$$

The quantization noise is uniformly distributed between $-\dfrac{V_{max}}{2^{b+1}}$ and $\dfrac{V_{max}}{2^{b+1}}$, and its standard deviation is

$$\sigma = \frac{V_{max}^2}{12 \times 2^{2b}} . \tag{5}$$

Because the quantization noise can be seen as a small disturbance over the infrared response voltage, its root-mean-square voltage is

$$V_{Qn0}^2 = \sigma = \frac{V_{max}^2}{12 \times 2^{2b}} \tag{6}$$
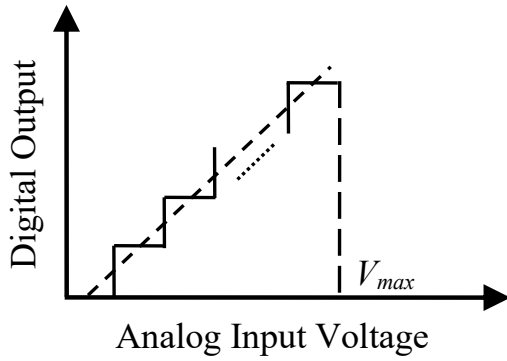
Fig. 3. The relationship between digital output and analog input

If the noise current is presumed as unit step function $\varepsilon(t)$, the noise integration voltage across the integration capacitor is

$$V_n = \frac{t}{C} \times [\varepsilon(t) - \varepsilon(t - t_{int})], \tag{7}$$

The noise output-input ratio of the photo-generated current integration circuit is

$$R_n = \frac{\frac{t}{C} \times [\varepsilon(t) - \varepsilon(t - t_{int})]}{\varepsilon(t)} . \tag{8}$$

Using the Laplace and Euler transforms [20], the noise upper cut-off frequency is

$$f_2 = \frac{1}{2t_{int}} . \tag{9}$$

In a similar way [12], the noise lower cut-off frequency is

$$f_1 = \frac{1}{4t_{stare}} , \tag{10}$$

where t_{stare} is the staring time of the focal plane array.

Thus, the Johnson and 1/f noise voltages on the integration capacitor can be obtained from equations (1), (2), (9), and (10) as

$$V_J^2 = \frac{2KT}{\pi RC} \ln \frac{2t_{stare}}{t_{int}} , \tag{11}$$

and

$$V_{1/f}^2 = \frac{V_v^2 k}{2\pi R^2 C} (4t_{stare} - 2t_{int}) , \tag{12}$$

2.2. Responsivity analysis

The infrared current responsivity of the microbolometer [15,21] is

$$R_I = \frac{V_b \alpha}{g(R + V_b^2 \alpha)} , \tag{13}$$

where α is the microbolometric temperature coefficient of resistance, and g is the thermal conductance of the microbolometer. Then, the infrared voltage responsivity of the microbolometer Fig. 2 can be deduced as

$$R_V = \frac{V_b \alpha t_{int}}{gC(R + V_b^2 \alpha)} . \tag{14}$$

2.3. Theoretical signal-to-noise ratio

If the absorbed infrared irradiation power of the microbolometer is Q, the signal-to-noise ratio is

$$SNR = \frac{R_V Q}{\sqrt{V_J^2 + V_{1/f}^2 + V_{Qn0}^2}} . \tag{15}$$

From equations (6), (11), (12), (14), and (15), the theoretical signal-to-noise ratio can be gotten as

$$\frac{QV_b \alpha t_{int}}{g(R + V_b^2 \alpha)\sqrt{\dfrac{2KTC}{\pi R} \ln \dfrac{2t_{stare}}{t_{int}} + \dfrac{V_v^2 kC}{2\pi R^2}(4t_{stare} - 2t_{int}) + \dfrac{C^2 V_{max}^2}{12 \times 2^{2b}}}} . \tag{16}$$

From the above equation, it can be obviously found that the increase of the integration time t_{int} and the decrease of the integration capacitor C can effectively improve the signal-to-noise ratio of the microbolometer. However, the small integration capacitor inevitably leads to high noise in the light of equations (11) and (12), although suitable for high-resolution small-sized pixel. In addition,

the larger integration time means the lower noise from equations (11) and (12), but the larger integration time can easily cause the voltage saturation of the integration capacitor.

3. Optimized digital readout integrated circuit

For next-generation microbolometric focal plane array with high-performance characteristics such as small-sized pixel, low-noise and high signal-to-noise ratio, an optimized digital CMOS readout integrated circuit is proposed in Fig. 4, in which the reference voltage V connected to the inverting input terminal of the comparator Com is larger than the voltage V_b. If the infrared response voltage on the integration capacitor reaches $V - V_b$, the comparator produces a count clock pulse to the counter and to form a reset signal for the reset switch S_0. Within the effective time of the row selecting signal, the counting value of the clock pulses of the comparator is the infrared response digital output D_{out}.
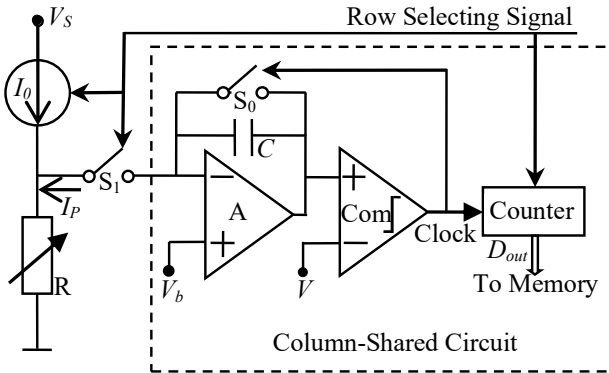

Fig. 4. Optimized digital readout integrated circuit

Based on the above introduction, $V - V_b$ is the quantization precision of the infrared response voltage. The quantization noise is uniformly distributed from 0 to $V - V_b$, and its root-mean-square voltage is

$$V_{Qn1}^2 = \frac{(V - V_b)^2}{12}.$$ (17)

Assumed the quantization precision is

$$q = V - V_b = \frac{V_{max}}{2^b},$$ (18)

the quantization noises of the conventional and optimized digital readout integrated circuits are the same as

$$V_{Qn}^2 = \frac{q^2}{12}.$$ (19)

Thus, the theoretical signal-to-noise ratio can be changed into

$$\frac{Q V_b \alpha t_{int}}{g(R + V_b^2 \alpha)\sqrt{\dfrac{2KTC}{\pi R} \ln \dfrac{2t_{stare}}{t_{int}} + \dfrac{V_v^2 kC}{2\pi R^2}(4t_{stare} - 2t_{int}) + \dfrac{C^2 q^2}{12}}}.$$ (20)

In short, it can be said that the proposed digital CMOS readout integrated circuit can significantly improve the integration time without changing other conditions. The improvement of the integration time can not only upgrade signal-to-noise ratio but also reduce noise while not causing the voltage saturation of the photo-generated current integration capacitor. Within the integration time, the infrared response signal is digitalized by the proposed digital readout integrated circuit with pulse frequency modulation not conventional pulse width modulation, and this means that the integration capacitor is charged and discharged multiple times during the integration time. Comparatively, the integration capacitor in conventional digital readout integrated circuit is only charged and discharged once during the integration time. The proposed digital CMOS readout integrated circuit has been successfully applied to an experimental microbolometric focal plane array, and its test results verify its excellent performance characteristics including low noise and infrared voltage responsivity, which will be introduced in another our paper.

4. Conclusions

The theoretical signal-to-noise ratio for microbolometric focal plane array with digital CMOS readout integrated circuit is given out basing on three certain of noise expressions and the microbolometric theoretical infrared voltage responsivity. According to the theoretical signal-to-noise ratio, a new kind of digital CMOS readout integrated circuit is proposed in this paper. The integration capacitor in the proposed digital CMOS readout integrated circuit can be repeatedly charged and discharged to form a list of counting clock pulses during a certain of integration time, the total pulse-counting value is the digitalized output of the infrared response voltage. This kind of digital CMOS readout integrated circuit can significantly increase the integration time without the integration capacitor saturation, which is favorable to the microbolometric focal plane array with high performance characteristics such as low noise, small-sized pixel, and high signal-to-noise ratio.

Acknowledgments

References

[1] M. A. Gülden, E. Zencir, E. Avu, Integration **82**, 14(2022).

[2] S. Yu, Y. Zhang, Y. Niu, Y. Zhou, Y. Zhuo, D. Ma, W. Lu, Z. Chen, X. Li, Journal of Infrared and Millimeter Waves **41**(4), 785 (2022).

[3] C. Wang, G. Song, Laser and Infrared **47**(8), 927 (2017).

[4] C. Lamsal, N.M. Ravindra, Emerging Materials Research **3**(4), 194 (2014).

[5] L. Yu, L. Tang Libin, W. Yang, Q. Qun, Infrared and Laser Engineering **50**(1), 202110131 (2021).

[6] C. C. Hsieh, C. Y. Wu, F. W. Jih, T. P. Sun, IEEE Transactions on Circuits & Systems for Video Technology **7**(4), 594 (1997).

[7] M. F. Snoeij, A. J. P. Theuwissen, K. A. A. Makinwa, J. H. Huijsing, IEEE Journal of Solid-State Circuits **42**(12), 2968 (2007).

[8] R. A. Wood, N. A. Foss, Laser Focus World **29**(6), 101 (1996).

[9] P. L. Richards, Journal of Applied Physics **76**(1), 1 (1994).

[10] L. A. McIlrath, IEEE Journal of Solid-State Circuits **36**(5), 846 (2001).

[11] A. Kitchen, A. Bermak, A. Bouzerdoum, IEEE Transactions on Electron Devices **52**(12), 2591 (2005).

[12] X. Chen, H. Zhao, C. Fang, Q. Lv, L. Chen, Optik - International Journal for Light and Electron Optics **219**, 165118 (2020).

[13] M. D. Ker, J. S. Chen, IEEE Transactions on Device and Materials Reliability **8**(2), 394 (2008).

[14] J. F. Johnson, IEEE Transactions on Electron Devices **46**(1), 96 (1999).

[15] R. A. Wood, Monolithic silicon microbolometer arrays, in: P.W. Kruse, D.D. Skatrud (Eds.), Uncooled Infrare Imaging Systems and Arrays, Academic Press, Smith, New York, 59 (1997).

[16] X. Chen, H. Zhao, C. Fang, Q. Lv, L. Chen, Optik - International Journal for Light and Electron Optics **219**, 165118 (2020).

[17] X. Chen, Q. Lv, X. Yi, Optik - International Journal for Light and Electron Optics **122** (23), 2143 (2011).

[18] X. Chen, C. Fang, Q. Lv, Optik - International Journal for Light and Electron Optics **177**, 21 (2019).

[19] X. Chen, Optik - International Journal for Light and Electron Optics **122**(9), 792 (2011).

[20] X. Chen, C. Fang, Q. Lv, R. Yang, Optik - International Journal for Light and Electron Optics **170**, 452 (2018).

[21] X. Chen, Q. Lv, Optical Engineering **54**(6), 063105 (2015).

_____

*Corresponding author: cxqdhl@sina.cn